IAI Journals.ASM.org

Neurons Are Host Cells for *Mycobacterium tuberculosis*

Philippa J. Randall,[a] Nai-Jen Hsu,[a] Dirk Lang,[b] Susan Cooper,[b] Boipelo Sebesho,[a] Nasiema Allie,[a] Roanne Keeton,[a] Ngiambudulu M. Francisco,[a] Sumayah Salie,[a] Antoinette Labuschagné,[a] Valerie Quesniaux,[c] Bernhard Ryffel,[c] Lauriston Kellaway,[b] Muazzam Jacobs[a,d]

Division of Immunology, Institute of Infectious Disease and Molecular Medicine, Health Sciences Faculty, University of Cape Town, Cape Town, South Africa[a]; Department of Human Biology, Health Sciences Faculty, University of Cape Town, Cape Town, South Africa[b]; University of Orleans and CNRS UMR7355, Experimental and Molecular Immunology and Neurogenetics, Orleans, France[c]; National Health Laboratory Service, Johannesburg, South Africa[d]

***Mycobacterium tuberculosis* infection of the central nervous system is thought to be initiated once the bacilli have breached the blood brain barrier and are phagocytosed, primarily by microglial cells. In this study, the interactions of *M. tuberculosis* with neurons *in vitro* and *in vivo* were investigated. The data obtained demonstrate that neurons can act as host cells for *M. tuberculosis*. *M. tuberculosis* bacilli were internalized by murine neuronal cultured cells in a time-dependent manner after exposure, with superior uptake by HT22 cells compared to Neuro-2a cells (17.7% versus 9.8%). Internalization of *M. tuberculosis* bacilli by human SK-N-SH cultured neurons suggested the clinical relevance of the findings. Moreover, primary murine hippocampus-derived neuronal cultures could similarly internalize *M. tuberculosis*. Internalized *M. tuberculosis* bacilli represented a productive infection with retention of bacterial viability and replicative potential, increasing 2- to 4-fold within 48 h. *M. tuberculosis* bacillus infection of neurons was confirmed *in vivo* in the brains of C57BL/6 mice after intracerebral challenge. This study, therefore, demonstrates neurons as potential new target cells for *M. tuberculosis* within the central nervous system.**

Tuberculosis is primarily a respiratory disease that is initiated after the inhalation of only a few bacilli and subsequent phagocytosis by alveolar macrophages to establish a local infection focus. Globally, approximately 8.8 million new cases of tuberculosis were reported in 2011, and the disease was associated with 1.45 million deaths (1). Although pulmonary tuberculosis is the predominant form of infection, extrapulmonary tuberculosis constitutes up to 20% of reported cases, approximately 1 to 5% of which are attributed to tuberculosis of the central nervous system (CNS-TB) (2). CNS-TB occurs primarily in childhood but significantly increases in adults under conditions of immune suppression, which are associated with considerable morbidity and mortality (3, 4). Pathogenesis of CNS-TB is initiated as a secondary infection during hematogenous dissemination of pulmonary infection to the brain parenchyma (5). Despite its neuroprotective properties, it has been proposed that *Mycobacterium tuberculosis* can cross the blood brain barrier and invade the CNS as free bacilli, which is supported by studies that illustrated pathogen-specific gene upregulation associated with traversal of the blood brain barrier (6). However, the mechanisms associated with evading the protective properties of the blood brain barrier for several bacteria, including *M. tuberculosis*, remain primarily undefined. Initial events during CNS-TB are characterized by infection of the meninges, the establishment of localized foci, and the subsequent release of bacilli into the subarachnoid space (7).

Several studies have investigated and reported on different cell types that are targeted by *M. tuberculosis* bacilli for invasion (8, 9, 10, 11). Among these, macrophages are well described as preferred host cells despite their primary protective function in innate immune responses; the evolutionary development of specific immune evasion mechanisms allows *M. tuberculosis* to exist within what is essentially a hostile environment. Studies have also indicated that cells other than macrophages, such as dendritic cells, are infected by *M. tuberculosis* bacilli at a higher rate than was previously thought (11). Differential cytokine profiles produced by infected macrophages and dendritic cells in comparative studies have suggested that the functional consequences of *M. tuberculosis* infection of these two distinct cell types may be different (12, 13). Similarly, *M. tuberculosis* infection of different nonphagocytic cell types may induce responses that are variable. The diversity of cell types that can be infected by *M. tuberculosis* bacilli, particularly at extrapulmonary sites, suggests that latent infection may be established at such locations. Recent studies demonstrated viable bacilli present in resident macrophages and sinusoidal endothelium cells of the spleen and liver expressing a genetic profile corresponding to latent infection (14).

M. tuberculosis bacilli encode specific proteins that actively facilitate entry into cells (15, 16), thereby circumventing the requirement for cells to be phagocytic in order to establish infection. Among several intracellular bacterial species that are capable of infecting the central nervous system (17), studies have indicated that microglia are targeted by invading *M. tuberculosis* bacilli (18, 19), leading to a robust proinflammatory response dependent on NADPH oxidase-dependent reactive oxygen species (ROS) generation (20) and the induction of reactive nitrogen intermediates (21). Neurons have never been shown to be infected by *M. tuberculosis* bacilli and are not thought to be involved in the etiology of the disease. However, neural targeting by *Mycobacterium leprae* through binding to laminin α2 on Schwann cells has been reported (22), and the presence of *M. leprae* in the medulla oblongata and spinal cord of patients with lepromatous leprosy was

Received 16 April 2013 **Returned for modification** 23 May 2013
Accepted 15 February 2014
Published ahead of print 24 February 2014
Editor: J. A. Appleton
Address correspondence to Muazzam Jacobs, Muazzam.Jacobs@uct.ac.za.
P.J.R. and N.-J.H. contributed equally to the study.

doi:10.1128/IAI.00474-13

inferred from DNA amplification studies, although the presence of bacilli within neurons was not detected (23). Nonetheless, several pathogenic species do infect neurons, including the intracellular bacterium *Listeria monocytogenes*, which can be controlled in a gamma interferon (IFN-γ)-dependent bactericidal manner (24, 25).

In this study, the potential of *M. tuberculosis* bacilli to infect neurons was investigated. Although neurons are generally regarded as nonphagocytic cells, Bowen et al. demonstrated that phagocytosis by different neuronal cell types occurs both *in vitro* and *in vivo* (26). The phagocytic capability of neurons may therefore be largely unappreciated and underinvestigated. Thus, it was hypothesized that neurons are capable of mycobacterial internalization, thereby affecting neuronal cellular responses. The results obtained in this study conclusively established that *M. tuberculosis* bacilli were able to infect neurons directly, as demonstrated by the intracellular location of bacilli through confocal microscopy.

MATERIALS AND METHODS

Mice. C57BL/6 mice were bred and maintained under specific-pathogen-free conditions at the animal facility of the University of Cape Town (South Africa). One-day-old neonates and adult mice between 8 and 12 weeks of age were used. All animal experimental protocols complied with South African regulations. Approval was obtained from the Animal Research Ethics Committee, University of Cape Town, Cape Town, South Africa (reference numbers AEC 010/017 and AEC 010/018) in accordance with the South African National Standard 10386, *The Care and Use of Animals for Scientific Purposes*.

Mycobacteria. *M. tuberculosis* strain H37Rv (Trudeau Mycobacterial Culture Collection, New York, NY), was grown at 37°C in Middlebrook 7H9 broth (Difco Laboratories) containing 10% oleic acid-albumin-dextrose-catalase (OADC) and 0.5% Tween 80 until log phase and then aliquoted and stored at −80°C. A frozen aliquot was thawed, passed 30 times through a 29-gauge needle, and plated in 10-fold serial dilutions on Middlebrook 7H10 agar (Difco Laboratories) containing 10% OADC and 0.5% glycerol. The concentration of *M. tuberculosis* was then determined by counting the CFU. *M. tuberculosis* with green fluorescent protein (H37Rv-GFP; provided by Joel Ernst, New York University School of Medicine, USA) was prepared similarly, with 25 μg/ml kanamycin added to broth or agar (11).

Cell cultures and infection. Primary microglia were isolated from mixed glial cultures prepared from cerebral cortices of C57BL/6 neonates of either sex, as described previously (27, 28). Cultures of mouse primary neurons were prepared from C57BL/6 day 17 embryos or neonates as described previously with modifications (29, 30, 31). Briefly, the dissected hippocampi were digested, dissociated by trituration, and then seeded at a density of 1×10^5 cells per well on poly-L-lysine-coated coverslips in 24-well plates or glass chamber slides. The primary neuronal cultures were maintained in serum-free neurobasal medium (Gibco) containing 2% B27 supplement (Gibco) at 37°C in a 5% CO_2 incubator.

HT22 (a murine neuronal cell line) was obtained from the Salk Institute, San Diego, CA, USA; Neuro-2a (murine neuroblastoma) and BV2 (murine microglia) cells were obtained from the National Institute for Cancer Research, Genoa, Italy. HT22 and Neuro-2a cells were propagated in Dulbecco's modified Eagle's medium (DMEM) with 10% fetal bovine serum (FBS), and BV2 cells were propagated in RPMI 1640 medium with 10% FBS. Human neuroblastoma SK-N-SH cells (a gift from A. Vahidnia, Leiden University Medical Centre, Leiden, Netherlands) were grown in DMEM supplemented with 10% FBS and differentiated for 2 weeks in culture with 10 μM retinoic acid (Sigma) (32).

To assess optimal cellular infection, neurons were seeded at 1×10^5/well, while microglia were seeded at 1×10^4/well, and cultured with *M. tuberculosis* at a multiplicity of infection (MOI) of 2:1, 5:1, 10:1, 30:1, 50:1, or 100:1 (ratios of *M. tuberculosis* bacilli to cells). Although association of *M. tuberculosis* with cultured neuronal cells occurred at all ratios (data not shown), an MOI of 30:1 was deemed optimal, supported by other studies using an *ex vivo* model of hippocampal neuronal infection with *L. monocytogenes* (25), while an MOI of 2:1 was found optimal for microglial infection. Thus, briefly, HT22 and Neuro-2a cells and primary hippocampal neurons were infected with H37Rv-GFP at an MOI of 30:1 and microglia at an MOI of 2:1 for 4 h in 24-well culture plates, after which the culture medium was replaced with fresh medium containing 50 μg/ml gentamicin (Sigma). For image studies, cells were fixed for staining at 6 h, 24 h, and 48 h postinfection for further analysis. For colony enumeration, neurons were extensively washed with phosphate-buffered saline (PBS) and lysed with 1% Triton X-100 in PBS, and the lysates were cultured on Middlebrook 7H10 agar (Difco) supplemented with 10% OADC, 0.5% glycerol, and 25 μg/ml kanamycin. Mycobacterial cultures were incubated inside semisealed plastic bags at 37°C for 18 to 21 days, and colony counts were registered.

Histology and immunocytochemistry of infected cultures. For histology, H37Rv-infected cells were fixed with 4% paraformaldehyde (PFA) in PBS, washed, and subjected to Ziehl-Neelsen (ZN) staining for acid-fast bacilli. For immunohistochemical analysis, H37Rv-GFP-infected cells were fixed with 4% PFA, washed, and blocked with 1% bovine serum albumin (BSA) and then incubated with either Alexa 555-conjugated phalloidin (1:600; Invitrogen) or anti-microtubule-associated protein 2 (MAP2) (1:1,000; Abcam) and visualized with Cy3-conjugated secondary antibody (1:1,000; Jackson ImmunoResearch Laboratories). SK-N-SH cell nuclei were stained with 6-diamidino-phenylidone (DAPI) (Sigma). The immunofluorescence-labeled cultures were mounted in fluorescent mounting medium (Dako), and images were captured with a Zeiss (Oberkochen, Germany) LSM 510 confocal microscope. High-resolution confocal imaging was carried out using a 63× (1.4-numerical-aperture [NA]) oil immersion objective, and z-stacks were acquired using Nyquist sampling parameters.

The quantification of *M. tuberculosis*-associated cultured cells was performed using light microscopy, where 100 to 400 microglial or neuronal cells were examined under bright-field microscopy for each experiment. Cultured neurons or microglia, which associated with *M. tuberculosis* bacilli, were calculated as the number of cells associated with acid-fast bacilli out of the total number of cells examined.

The quantification of cells that contained internalized *M. tuberculosis* bacilli was performed using confocal microscopy, where 100 to 150 cells per cell type were examined for each experiment. The cells containing internalized bacilli were counted in the 3-dimensional z-stack images of 5 different fields per cell type. The percentage of internalization was calculated as the number of cells containing intracellular H37Rv-GFP bacilli out of the total number of cells counted in the z-stack images.

Intracerebral infection and immunohistochemistry of infected mice. Six C57BL/6 female mice (8 to 12 weeks old) from 2 independent experiments were inoculated intracerebrally in the left cerebral hemisphere with 1×10^5 CFU of H37Rv-GFP using a Hamilton syringe (Gastight no. 1701; Hamilton, Bonaduz, Switzerland). At 7 and 14 days postinfection, the infected mice were deeply anesthetized and transcardially perfused with 4% PFA. The 40-μm brain sections were cut using a vibratome and then processed for immunohistochemistry. The microglia and astrocytes were labeled with CD11b (clone M1/70; 1:500; Abcam) and glial-fibrillary acidic protein (GFAP) antibody (1:1,000; Sigma), respectively. The neurons were labeled with either NeuN (clone A60; 1:100; Merck-Millipore), MAP2 (1:1,000; Abcam), or β-III-tubulin antibody (1:1,000; Abcam) and corresponding Cy3-conjugated secondary antibodies (Jackson ImmunoResearch Laboratories). The nuclei were stained with DAPI (Sigma). The immunofluorescence-labeled sections were mounted in fluorescent mounting medium and viewed with a Zeiss 510LSM unit.

Lysotracker staining. To effectively label and track phagolysosomes in live cells, infected cultures were incubated with Lysotracker (Molecular Probes, USA) before fixation and permeabilization. Two hours prior to the experimental time points, Lysotracker (1:900) was added to the cul-

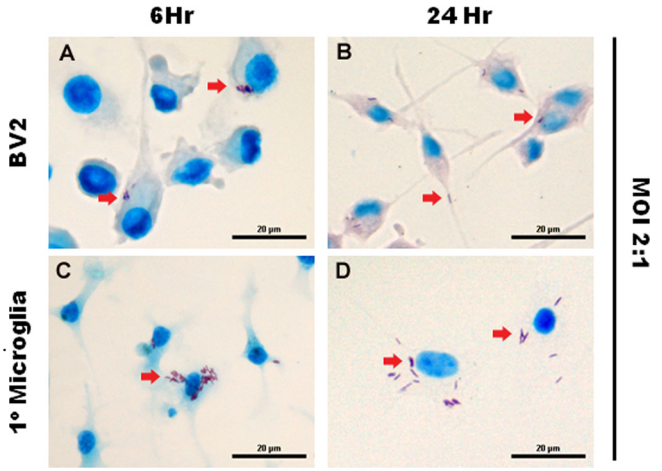

FIG 1 *M. tuberculosis* infects microglia. The microglial cell line BV2 (A and B) and primary microglia (C and D), isolated from the cortices of 1-day-old C57BL/6 neonates, were infected with *M. tuberculosis* at an MOI of 2:1 for 6 and 24 h. The arrows indicate the uptake of acid-fast bacilli by the microglial cells. Scale bars, 20 μm

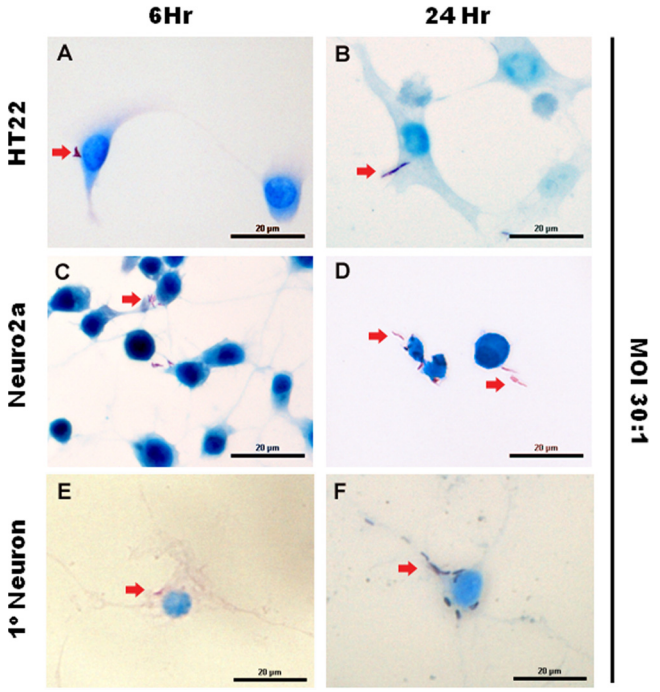

FIG 2 *M. tuberculosis* bacilli are associated with cultured neurons. Neuronal cultures—HT22, Neuro-2a, and primary neurons—established from the hippocampi of 1-day-old C57BL/6 neonates were infected with *M. tuberculosis* at an MOI of 30:1 for 6 and 24 h. Ziehl-Neelsen staining shows the presence of acid-fast bacilli (arrows) in the cytoplasm and neurites of neurons. Scale bars, 20 μm.

ture supernatant at 37°C. At 24 h or 48 h postinfection, the cells were fixed with 4% PFA in PBS, washed, and blocked with 1% BSA in PBS. To ensure sufficient staining, the cells were incubated again with Lysotracker (1:1,000) overnight at 4°C. Subsequently, nuclei were stained with DAPI, and the coverslips were mounted in fluorescent mounting medium (Dako, CA, USA).

Cytokine quantification. Supernatants from neuronal cultures were frozen at −80°C until further analysis. Cytokine concentrations were determined by enzyme-linked immunosorbent assay (ELISA) using reagents from R&D Systems (Minneapolis, MN) according to the instructions of the manufacturers.

Statistical analysis. The data are presented as means and standard deviations (SD). Statistical analysis was performed by one-way analysis of variance (ANOVA) and one-tailed *t* test for comparisons among the time points. For all tests, a *P* value of <0.05 was considered significant.

RESULTS

***M. tuberculosis* bacilli associate with neuronal cultures.** In initial studies, the microglial cell line BV2 and cortex-derived primary microglia were cultured in the presence of *M. tuberculosis* bacilli at an MOI of 2:1 for 6 h, 24 h, and 48 h as established phagocytic cells against which to measure neuron-bacillus interaction. A time-dependent association of *M. tuberculosis* bacilli was observed in both BV2 (Fig. 1A and B) and primary microglial (Fig. 1C and D) cultures with >30% of host cells representing microglia-bacillus interaction. Next, neuronal cultures of immortalized HT22 cells (Fig. 2A and B) and Neuro-2a cells (Fig. 2C and D) were exposed to *M. tuberculosis* bacilli at an MOI of 30:1 for 6 h, 24 h, and 48 h. Analysis of infected neuronal cultures showed that *M. tuberculosis* bacilli were associated with the soma and the neurites. Quantitatively, there was a time-dependent increase in association of *M. tuberculosis* bacilli with both neuronal cell lines and an overall higher number of HT22 cells than of Neuro-2a cells associated with bacilli at all time points investigated (Table 1). Although Neuro-2a cells and HT22 cells are widely used to characterize neuronal behavior and responses, in general, transformed cell lines may differ from primary cells with respect to structure, development, binding, and functional characteristics (33). Therefore, to confirm the neuronal infectivity of *M. tuberculosis* bacilli and to exclude the possibility that previously observed mycobacterial association was due to anomalous characteristics of neuronal cell lines, the observation was validated in primary neuronal cell cultures. Primary neuronal cell cultures were established from murine hippocampi and infected with *M. tuberculosis* bacilli at an MOI of 30:1 for 6 h, 24 h, and 48 h. Uptake in primary neuronal cultures was comparable to that in HT22 cells and Neuro-2a cells; *M. tuberculosis* bacilli displayed a time-dependent increase in association from 7.9% to 21.3% over a 48-h period (Table 1) with bacilli associated with the neurites and cell bodies (Fig. 2E and F). Therefore, for the first time, the data clearly demonstrate that *M. tuberculosis* is capable of direct interaction with neurons.

Murine neurons internalize *M. tuberculosis* bacilli *in vitro*. Observations of an association of bacilli with cultured neurons after Ziehl-Neelsen staining may have represented bound extracellular bacilli rather than bacteria that were intracellular. To investigate whether *M. tuberculosis* bacilli were indeed internalized by neurons, the neuronal cell lines HT22 (Fig. 3A to C) and Neuro-2a (Fig. 3D to F), as well as primary neuronal cultures (Fig. 3G to I), were infected with a recombinant GFP-expressing *M. tuberculosis* H37Rv strain at an MOI of 30:1. Similarly, BV2 microglial cells (Fig. 3J to L) were infected at an MOI of 2:1 to act as a positive-control cell strain for bacterial internalization. To confirm cytoplasmic localization of bacilli in microglia, the cultures were stained with cytofluorochrome-conjugated phalloidin, a cytoskeletal marker, and analyzed by confocal microscopy. Analysis of z-stack images showed that in most cases multiple bacilli were phagocytosed by BV2 (Fig. 3K), and orthogonal views confirmed that all bacilli were internalized (Fig. 3L). To determine

TABLE 1 Microglial and neuronal association and internalization of *M. tuberculosis* bacilli[a]

Cell type	Bacillus/ cell ratio	% cell associated			% internalized		Ratio (% internalized/% cell associated)	
		6 h	24 h	48 h	24 h	48 h	24 h	48 h
BV2	2:1	2.1 ± 0.92	31.1 ± 1.84	34.6 ± 4.79	31.0 ± 4.20	34.7 ± 2.50	1.00	1.00
Primary microglia	2:1	6.5 ± 2.23	31.5 ± 5.83	32.5 ± 0.86	30.8 ± 6.30	32.1 ± 6.56	0.98	0.99
HT22	30:1	6.7 ± 1.65	17.2 ± 9.74	28.9 ± 1.00	11.8 ± 1.83	17.7 ± 1.34	0.68	0.61
Neuro-2a	30:1	1.9 ± 0.45	6.1 ± 4.03	20.0 ± 0.72	6.2 ± 1.41	9.8 ± 1.97	1.00	0.49
Primary neurons	30:1	7.9 ± 1.64	13.6 ± 3.30	21.3 ± 0.46	11.2 ± 0.89	10.1 ± 2.07	0.82	0.48
SK-N-SH	30:1	10.2 ± 1.47	17.9 ± 2.65	21.0 ± 2.41	11.9 ± 1.72	18.5 ± 1.18	0.67	0.88

[a] Microglia and neurons were infected with *M. tuberculosis*, and cells that were associated with or had internalized bacilli at 6 h, 24 h, and 48 h were counted. The results represent the means ± SD of the combined data from at least 3 individual experiments.

whether *M. tuberculosis* bacilli were internalized by neurons, infected HT22 and Neuro-2a cultures were stained with cytofluorochrome-conjugated phalloidin while infected primary neurons were identified with the neuron-specific marker MAP2. The orthogonal display of the three-dimensional data demonstrated internalized *M. tuberculosis* bacilli in HT22 (Fig. 3C), Neuro-2a (Fig. 3F), and primary neuronal (Fig. 3I) cultures, embedded within cytoplasmic structures, as identified by the different markers.

Quantification of the cells with bacilli showed ≥98% of microglial-cell-associated bacilli were internalized after 24 h and 48 h (Table 1). Importantly, for HT22, 11.8% and 17.7% of cultured cells internalized *M. tuberculosis* bacilli after 24 h and 48 h, respectively (Table 1). Although Neuro-2a internalization was approximately 2 times lower than that of HT22, significant internalization levels of 6.2% and 9.8% at 24 h and 48 h were nonetheless measured (Table 1). For primary neuronal cultures, 11.2% of cells had internalized bacilli at 24 h, which decreased slightly to 10.1% after 48 h (Table 1). Overall, the relative ratios indicated that, whereas microglial cells internalized most of the associated bacilli, murine neuronal cells internalized only 45 to 65% of associated bacilli after 48 h (Table 1). Moreover, to determine whether internalized *M. tuberculosis* bacilli within neurons represent a productive infection, where bacilli remain viable and retain the capacity to replicate, infected HT22 and Neuro-2a cells and primary neurons were lysed at 6 h, 24 h, and 48 h, and bacterial colonies were enumerated. The data indicated that initial uptake and internalization of mycobacteria within primary neurons may be superior to those of HT22 and Neuro-2a, with significantly higher bacillus levels at 6 h (Fig. 3M). Notably, bacillus growth occurred in all neuron cultures, with significantly higher numbers recorded at 48 h than at 6 h (Fig. 3M).

Thus, the study provided evidence that neurons are capable of internalizing *M. tuberculosis* bacilli that are viable and capable of replication within the neurons.

Neurons internalize *M. tuberculosis* bacilli *in vivo*. In this study, the localization of GFP-expressing *M. tuberculosis* (green) in relation to two different intracellular neuron-specific markers, β-III-tubulin (red) and MAP2 (red), was analyzed, and the results were compared to microglial uptake. Orthogonal projections (Fig. 4B, D, and F) representing 3-dimensional data sets provide a view of the *x* and *y*, as well as the *z*, dimensions of the original z-stack. Cell nuclei were labeled with DAPI. The respective differential interference contract (DIC) images (Fig. 4A, C, and E) illustrate the position of *M. tuberculosis*-GFP within the tissue. From the data presented in Fig. 4B, it was clear that *M. tuberculosis*-GFP bacilli were contained within β-III-tubulin-positive neuronal structures (red), indicated by partial colocalization (yellow) of the red and green fluorescence signals. Similarly, bacilli resided within MAP2-positive neuronal structures (red), which resulted in a yellow colocalization signal (Fig. 4D). Green fluorescent bacilli were also present, although it was unclear whether they represented free or internalized bacilli where MAP2 did not condense around the bacillus, as limitations in optical resolution prevented the delineation of cellular structure. Microscopic observations indicated that $CD11b^+$ microglial cells contained higher numbers of bacilli than neurons. CD11b, as a cell surface antigen, allows sufficient spatial separation of the red signal on the surface and the green signal from the internalized bacilli not to result in a colocalized (yellow) signal, as clearly evident in Fig. 4F.

Therefore, the data demonstrate that *M. tuberculosis* bacilli can be internalized by neurons under both *in vitro* and *in vivo* conditions but that neuronal uptake is subordinate to that of microglia.

***M. tuberculosis* bacilli encapsulated within neuronal cytoskeletal structures.** To gain additional insight into the relationship between neuronal structures and internalized bacilli, localized cytoplasmic sites were further investigated *in vitro* and *in vivo*. Bacilli may display distinct condensation of cytoskeletal elements ($MAP2^+$) around them, which resulted in partial colocalization of the fluorescent signals (yellow) but still allowed separation of the structures *in vitro* (Fig. 5A). Figure 5B confirmed neuronal internalization of the bacillus, whereas closer inspection and analysis of detailed images (Fig. 5B1 to B3) revealed that the bacillus resided within a MAP2-positive capsule-like cytoplasmic neuronal structure indicative of rearrangement of the cytoskeleton during infection. Similarly, this colocalization was observed *in vivo*. As described above, in Fig. 4B and D, colocalization indicated *M. tuberculosis* infection of neurons within the CNS following intracerebral challenge. The scan resolution of these sections, due to background and tissue thickness (40 μm), was not sufficient to separate the red and green immunofluorescent signals from cytoplasmic markers and bacilli, respectively. However, the MAP2 image (Fig. 5D) showed MAP2 condensation within the area surrounding the bacillus. Therefore, it is plausible that the *in vivo* infection of neurons by *M. tuberculosis* (Fig. 5C to E) likely reflects conditions observed *in vitro* (Fig. 5B1 to B3).

Cultured human neuronal cells internalize *M. tuberculosis* bacilli. The data demonstrated *M. tuberculosis* internalization by murine-derived neuronal cell lines and primary murine neuronal cultures, which were confirmed by neuronal uptake *in vivo*. To ascertain whether these observations have clinical relevance, we

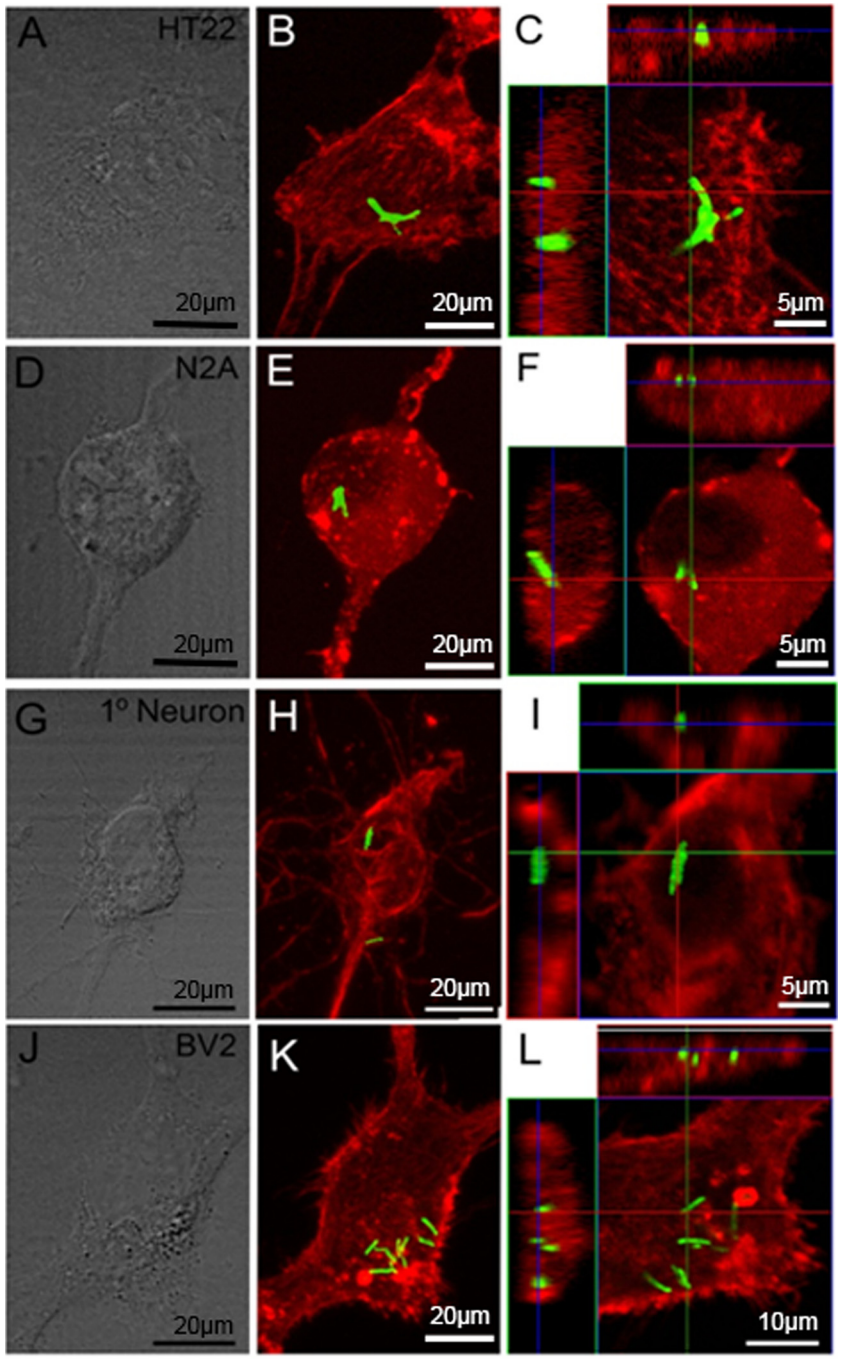
A
HT22
20μm
B
20μm
C
5μm
D
N2A
20μm
E
20μm
F
5μm
G
1° Neuron
20μm
H
20μm
I
5μm
J
BV2
20μm
K
20μm
L
10μm

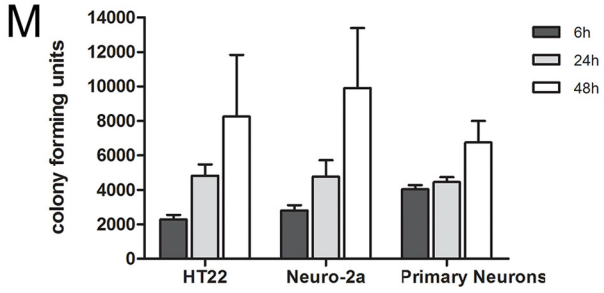
M
colony forming units
14000
12000
10000
8000
6000
4000
2000
0
HT22
Neuro-2a
Primary Neurons
6h
24h
48h

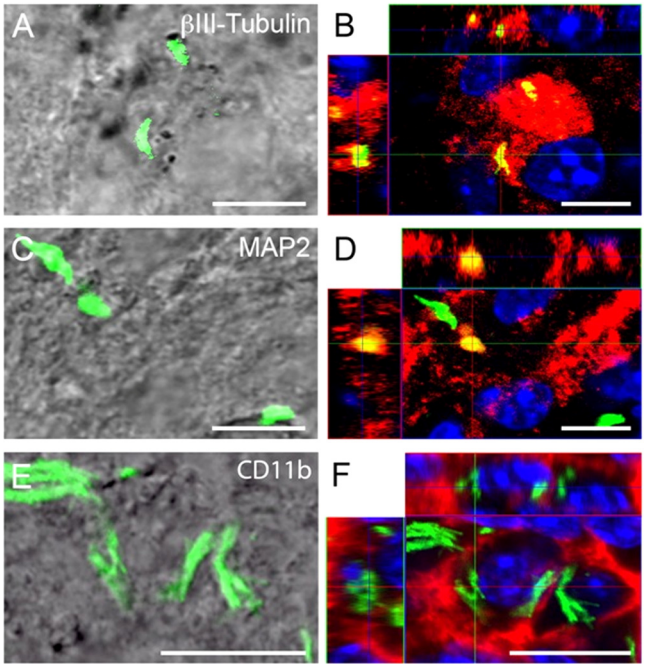

FIG 4 Confocal microscopy of internalized *M. tuberculosis* bacilli in neurons in brain sections of C57BL/6 mice 7 days after intracerebral infection. (B, D, and F) Orthogonal projections representing 3-dimensional data sets provide a view of the *x-y*, as well as the *z*, dimensions of the original z-stack. Cell nuclei are labeled with DAPI (blue). (A, C, and E) DIC images showing the tissue localization of H37Rv-GFP (green). (B) H37Rv-GFP bacilli are contained within β-III-tubulin-positive neuronal structures (red), indicated by partial colocalization (yellow) of the red and green fluorescence signals. (D) Bacilli are found within MAP2-positive neuronal structures (red, resulting in a yellow colocalization signal), but also disassociated from MAP2 (green). The latter may represent internalized or free bacilli, as it is not possible to delineate cell boundaries in these preparations. (F) Brain macrophages (identified by CD11b immunoreactivity) (red) contain large numbers of bacilli (green). CD11b is a cell surface antigen; therefore, no signal colocalization is observed. Scale bars, 10 μm.

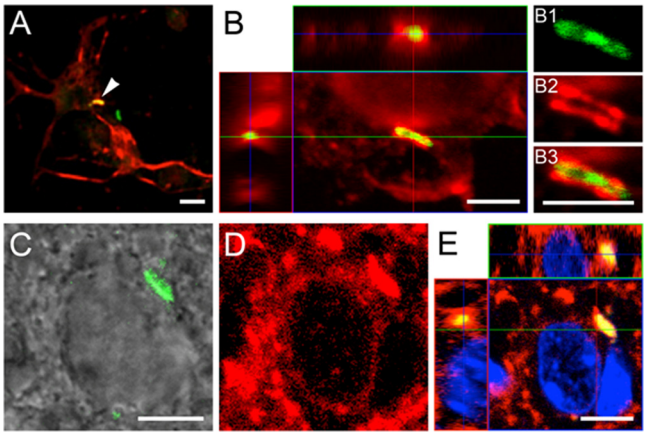

FIG 5 Confocal microscopy of internalized *M. tuberculosis* bacilli in cultured murine primary neurons and in brain sections. (B and E) Orthogonal projections representing 3-dimensional data sets provide a view of the *x-y*, as well as the *z*, dimensions of the original z-stack. Cell nuclei are labeled with DAPI (blue). (A) Overview of MAP2-positive neurons (red), established from the hippocampi of 17-day-old C57BL/6 mouse embryos, containing an H37Rv-GFP bacillus (arrowhead). (B) Bacilli (green) are found associated with MAP2-positive neuronal structures, such as the cortical cytoplasm and neurites (red), resulting in a partial colocalization signal (yellow). (B1 to B3) Detailed images reveal localization of the bacillus within the MAP2-positive neuronal structure. Panels A and B represent a 24-h time point. (C and D) In brain sections (14 days postinfection), colocalization of bacilli (green signal in DIC image) (C) and MAP2 signal (D) is evident (yellow signal in panel E), indicating internalization of bacilli by the neurons. However, it is not possible to resolve the relevant structures in brain sections at the level seen *in vitro*. Scale bars, 5 μm.

infected retinoic acid-differentiated SK-N-SH human-derived neuroblastoma cell cultures with *M. tuberculosis*-GFP bacilli at an MOI of 30:1. The cytoplasmic localization of fluorescent bacilli within SK-N-SH cultures was confirmed through staining with the neuron-specific marker β-III-tubulin or MAP2. Similar to the observations described for murine-derived neuronal cultures, the orthogonal display of the three-dimensional data demonstrated internalized *M. tuberculosis* bacilli in either β-III-tubulin-positive (Fig. 6C) or MAP2-positive (Fig. 6F) cytoplasmic structures. In addition, internalization was confirmed via the colocalization of the green (bacilli) and red (β-III-tubulin or MAP2) fluorescence signals, resulting in a partially yellow fluorescence signal (Fig. 6C and F). Quantification of the percentage of SK-N-SH cells associated with bacilli showed a statistically significant increase from 10.2% to 21% over 48 h (Table 1), similar to observations in murine-derived neuronal cultures. The percentage of cells that internalized bacilli increased from 11.9% to 18.5% from 24 h to 48 h (Table 1). This study therefore confirms that human neuronal cells are capable of being infected by *M. tuberculosis* bacilli.

Limited association of *M. tuberculosis* bacilli with phagolysosomes during neuronal infection. Previous studies have demonstrated that neurons are capable of phagocytosis (26), thereby introducing the possibility that *M. tuberculosis* bacilli may be internalized in this manner. We investigated the association of *M. tuberculosis* bacilli with phagolysosomes in primary neuronal cultures infected at an MOI of 30:1 for 24 h and 48 h. Analysis of confocal images showed predominant separation of the Lysotracker Red marker and green fluorescent bacilli, which indicated either arrest of phagosome-lysosome fusion during neuron infection or, alternatively, residence of bacilli within the cytosol and not within phagosomes (Fig. 7).

Neurons are activated during *M. tuberculosis* infection. Neurons are capable of generating an immune response when con-

FIG 3 Confocal microscopy of internalized *M. tuberculosis* bacilli and bacterial replication in neurons. HT22 cells (A to C), Neuro-2a cells (D to F), and primary neurons (G to I), established from the hippocampi of 17-day-old C57BL/6 mouse embryos, and BV2 cells (J to L) were infected with *M. tuberculosis* for 24 h and then subjected to immunohistochemistry for 6 h, 24 h, and 48 h, and the numbers of CFU were determined from lysed cultures (M). The fluorescence images of phalloidin-labeled cell lines, including HT22, Neuro-2a, and BV2, and MAP2-labeled primary neurons highlight the cytoskeletal proteins (red) to demonstrate the cytosolic location of GFP-expressing bacilli (green). The internalized bacilli can be seen in the top and side images in the orthogonal views, which show the colocalization of cytoskeleton and bacilli in the *x-y* plane of an optical section of the z-stack. Phase-contrast images of cultured cells are presented in panels A, D, G, and J. (M) Bacterial replication in HT22 and Neuro-2a cells and primary neurons assessed at 6 h, 24 h, and 48 h. The results are the means and SD of quadruple experimental data sets and are representative of one of three similar experiments.

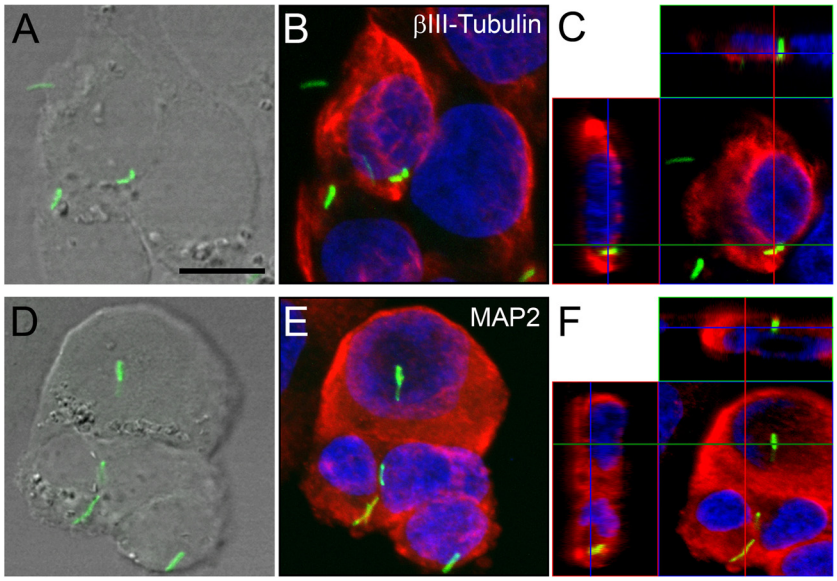

FIG 6 Confocal microscopy of internalized *M. tuberculosis* bacilli in human SK-N-SH cultured neurons. (B, C, E, and F) SK-N-SH cultured neurons labeled with anti-β-III-tubulin (B and C) and anti-MAP2 (E and F) antibodies (red). (B and E) Maximum-intensity projections of z-stacks of entire cells. (C and F) Orthogonal projections representing 3-dimensional data sets provide a view of defined optical sections in the *x-y*, as well as the *z*, dimensions of the original z-stack. Cell nuclei are labeled with DAPI (blue). (A and D) DIC images showing the tissue localization of H37Rv-GFP bacilli (green). Scale bar, 20 μM. The images represent neuronal cultures at 48 h.

fronted by various pathogens. However, neuronal activation in response to *M. tuberculosis* bacilli has not yet been reported. In this study, interleukin 1β (IL-1β), IL-6, and IL-10 cytokine expression was measured in *M. tuberculosis*-infected HT22 and Neuro-2a cells and primary neurons as an indication of functional response (Fig. 8). Both neuronal cell lines and primary neuronal cultures had significantly higher ($P < 0.05$) induction of the proinflammatory cytokines IL-1β and IL-6 and the anti-inflammatory cytokine IL-10 during exposure to *M. tuberculosis* bacilli after 48 h than uninfected cultures. IL-6 expression was higher than IL-1β or IL-10 levels measured in all cultures, with Neuro-2a cell synthesis being superior to that of HT22 or primary neuronal cultures. This study therefore, established that neurons have the capacity to induce an immune response during *M. tuberculosis* challenge.

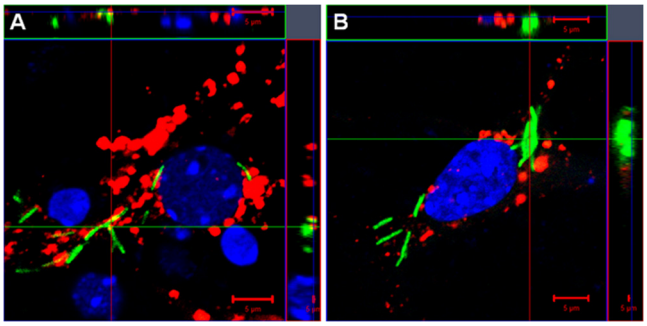

FIG 7 Limited association of *M. tuberculosis* bacilli with neuronal phagolysosomes. Murine primary neuron cultures were established from hippocampi of 17-day-old C57BL/6 embryos and infected with H37Rv-GFP bacilli (green) at a multiplicity of infection of 30:1. The neurons were stained with the phagolysosome marker Lysotracker (red) after 24 h (A) and 48 h (B). Cell nuclei were labeled with DAPI (blue) and analyzed by confocal microscopy. The images represent 3-dimensional data sets and provide a view of the *x-y* and *z* dimensions of the original z-stack. A colocalized signal (yellow) resulting from the association of the bacilli (green) with the phagolysosome, labeled with Lysotracker (red), is rarely observed in neurons at 24 h (A) and 48 h (B) postinfection, and most internalized bacilli appear disassociated from the phagolysosome. Scale bars, 5 μm.

DISCUSSION

Numerous bacterial species are able to invade the CNS to establish infection, and the mechanisms of invasion of several are known and their target cells identified (17). In contrast, the mechanisms associated with *M. tuberculosis* infection of the CNS and the specific cells targeted for invasion are mostly unknown. Although studies have described microglia as the preferred cell population infected by *M. tuberculosis* bacilli during CNS-TB pathogenesis (18, 19, 20), the ubiquitous nature of *M. tuberculosis* enables it to infect different cell types, which include both phagocytic and nonphagocytic cells (8, 9). Previous studies that investigated the relationship between *M. tuberculosis* bacilli and cells of the CNS have typically focused on microglia as the principal cellular target for infection (18, 34), while astroglia were infected to a lesser extent (19). The interaction of *M. tuberculosis* bacilli with neuronal cells has not yet been reported; hence, in a series of experiments, the neuronal infectivity of bacilli was investigated. This study describes the novel observation of neurons acting as additional target cells for *M. tuberculosis* bacilli in the CNS. It was demonstrated for the first time that, other than uptake by microglia and astrocytes, *M. tuberculosis* bacilli display neurotropic qualities and are internalized by neurons during CNS infection. Nonphysiological factors due to the immortalization of cell lines used in this study were excluded as contributing factors for bacillus uptake by demonstrating that *de novo* cultures of isolated primary neurons internalize *M. tuberculosis* bacilli. The physiological relevance of these findings was validated through *in vivo* infection studies, substan-

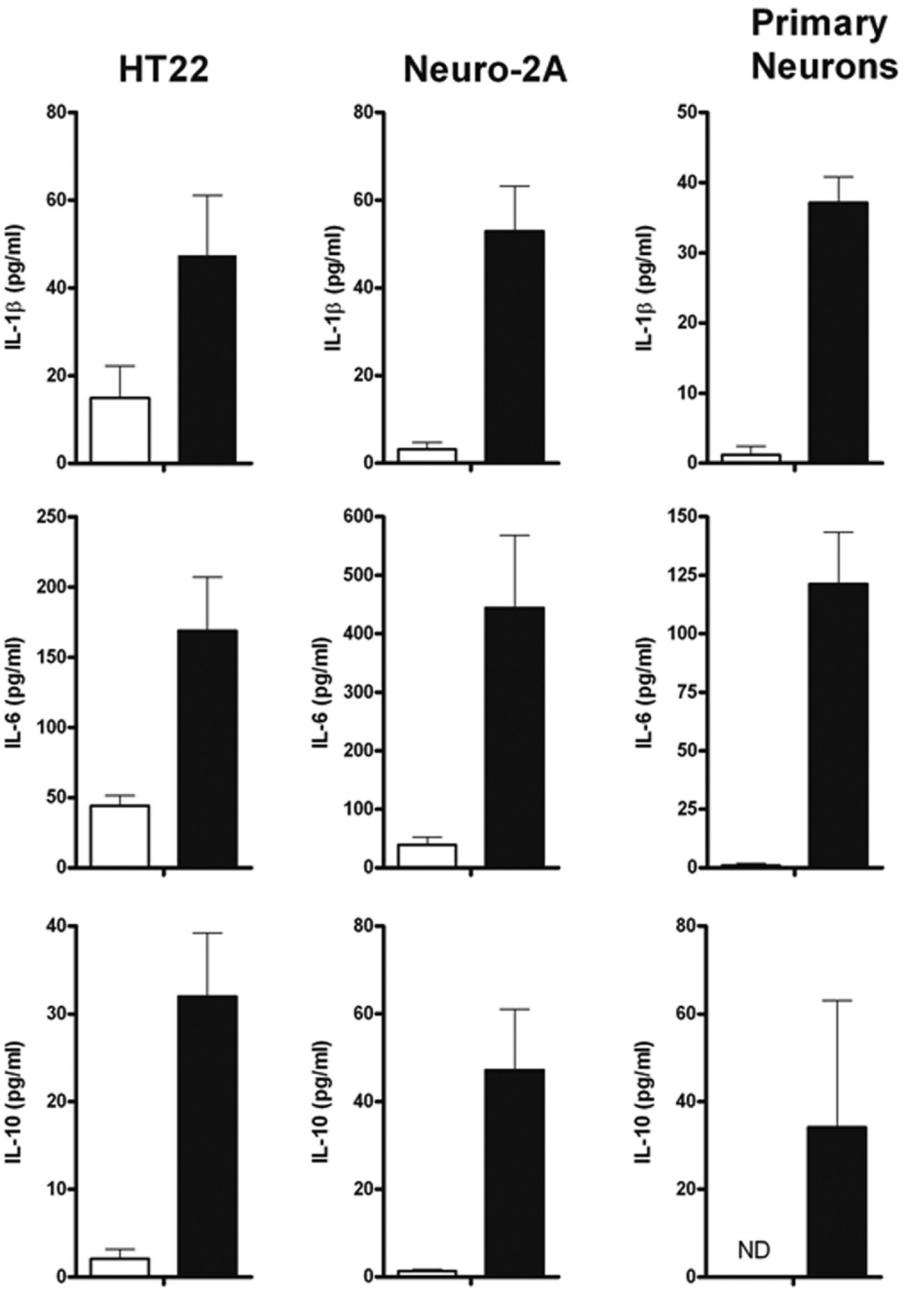

FIG 8 Neurons induce an immune response during *M. tuberculosis* infection. HT22, Neuro-2a, and primary neuronal cultures were infected with *M. tuberculosis*, and IL-1β, IL-6, and IL-10 were measured in the culture supernatants after 48 h by ELISA. The results represent the means and SD of combined data from 4 to 6 experiments; each experiment was performed in triplicate. ND, not detected.

tiating observations and conclusions from *in vitro* culture investigations.

This study demonstrates internalization of *M. tuberculosis* bacilli by neurons, although the manner in which pathogen recognition occurs is unknown. Neurons can be activated via innate immune pathways, commonly expressed in macrophages, where binding and recognition are mediated through cell surface-expressed molecules that include Fc receptors, mannose receptors, complement receptors, and Toll-like receptors (TLRs) (35). Here, neuronal expression of TLR2 and TLR4 (36, 37) may potentially present them as receptor candidates for bacillus recognition, as we and others have shown that both molecules are critical for protective immune function against *M. tuberculosis* bacilli (38, 39). However, their role is controversial, as reports have also shown redundancy for TL2 and TLR4 in mediating immune protection. Uptake of *M. tuberculosis* bacilli by mononuclear cells occurs primarily through phagocytosis. The phagocytic capacity of neurons is contentious, and while Bowen et al. (26) demonstrated that neurons are capable of phagocytosis, thereby elucidating a potential mechanism for neuronal entry of *M. tuberculosis* bacilli, other mechanisms of uptake require investigation. Our data showing that the majority of *M. tuberculosis* bacilli do not reside within

phagolysosomes of neurons suggest that mechanisms of entry other than phagocytosis should be considered, although it cannot be excluded. Indeed, entry of *M. tuberculosis* bacilli into other nonphagocytic cells indicates an active mechanism of invasion induced by the organism (8). The *M. tuberculosis* bacillus carries four mammalian cell entry (*mce*) operons, with mce1A potentially mediating invasion of host cells (15, 16).

The data presented in this study do not exclude phagocytosis as a mechanism through which bacilli are internalized, but the limited colocalization with acidified vesicles would then argue for arrest of phagolysosome maturation during neuronal infection. Alternatively, bacilli may be free within the cytoplasm, either through nonphagocytic entry or subsequent to phagosome escape, though the latter remains an area of controversy (40). Whether neurons employ macropinocytosis as a mechanism for *M. tuberculosis* bacillus uptake, as was shown in nonphagocytic cells (8), remains to be elucidated. Nevertheless, two populations of internalized bacilli could clearly be distinguished: those that colocalized with cytoskeletal structures and those that did not. Whether these two bacterial populations reside within different cytoplasmic environments or whether they represent different stages of the same internalization process is unclear. However, bacilli that were tightly associated with cytoplasmic structures within neurons appeared to be encased in a sheath-like structure, evidence of cytoskeletal rearrangement upon infection. *M. tuberculosis* bacillus-induced cytoskeletal rearrangement is known and has previously been reported (41, 42), and the observations in this study suggest that similar changes in the neuronal cytoskeleton occur during bacillus invasion. Moreover, it was established that entry of *M. tuberculosis* bacilli into epithelial cells was dependent on microtubules, which could be inhibited by administration of colchicine and nocodazole, known to cause microtubule depolymerization (43). Our findings do not exclude cytoskeletal concentration around bacilli residing within phagosomes, as others have shown actin nucleation around mycobacterial phagosomes (44, 45). The role of cytoskeletal concentration around bacilli is controversial, and its complexity is highlighted by contrasting reports. Kolonko and colleagues (45) suggest that actin polymerization protects *M. tuberculosis* bacilli from delivery to a bactericidal environment, whereas Anes and colleagues (44) propose that actin assembly promotes killing of pathogenic mycobacteria.

In this study, the overall capacity of neurons to internalize *M. tuberculosis* bacilli was reduced compared to microglial cells, reflected in the greater number of microglia than of neurons that were infected. In addition, generally fewer bacilli were internalized by neurons than by microglia in culture, despite being exposed to higher concentrations of bacilli. This is not surprising, as neurons are not considered to be professional phagocytic cells like microglia, and under normal conditions, preferential uptake is mediated by microglia. However, it may be argued that under conditions where the growth of bacilli is promoted, such as in HIV coinfection, where immune suppression prevails, *M. tuberculosis* infection of neurons could occur. The difference in uptake may represent variance in recognition of bacilli when exposed to either microglia or neurons, or it may reflect differences in the phagocytic capabilities of the cell types. Nonetheless, the increased capacity of microglia to phagocytose bacilli within an environment usually regarded as immune privileged can be interpreted as a protective role for microglia over neurons during CNS-TB. Indeed, evidence from several reports points to a cooperative relationship between microglia and neurons, where neuronal function is shielded by microglial activity (46). It is therefore interesting to speculate that direct targeting of neurons for infection could potentially represent an evasive mechanism by which bacilli circumvent the bactericidal effects of microglia. The evidence provided in this study indicates that the microenvironment present within neurons is permissive for bacterial replication and could potentially present a cellular niche for persistence. For example, a key mechanism of host protection against *M. tuberculosis* bacilli is apoptosis of infected cells mediated by cytolytic T cells (47). Reduced expression of major histocompatibility complex (MHC) class 1 in adult neurons (48) would favor escape from $CD8^+$ T cell-mediated apoptosis once the neurons are infected by *M. tuberculosis* bacilli and promote the cell type as a reservoir for persistence, as has been described for other cells in extrapulmonary tissues (14). Nonetheless, the data in this study, which show neurons to be capable of a functional cytokine response, may indicate integral involvement as part of the host collective immune reaction rather than acting as passive bystander cells during *M. tuberculosis* bacillus challenge.

Importantly, data that demonstrate the ability of *M. tuberculosis* bacilli to infect human neuronal cells provide a persuasive argument for neurons to be considered clinically important as potential host cells. Several studies have reported an increase in the prevalence of CNS-TB under conditions of immune suppression, e.g., in HIV-coinfected patients, who often present with low $CD4^+$ T cell counts (49, 50). *M. tuberculosis* bacilli are more likely to be detected in the cerebrospinal fluid (CSF) of immunosuppressed patients (51, 52), possibly due to higher levels of bacilli and of dissemination. As a key requirement to control *M. tuberculosis* bacillus replication (53), low $CD4^+$ T cell counts could predispose such patients to increased levels of CNS bacilli. Therefore, neuronal infection may be particularly relevant under clinical conditions where patients fail to control CNS-TB infection and the bacillus burden is substantial, possibly at specific, localized foci within the brain, and thereby potentially creates conditions for neurons to be targeted. Therefore, it is interesting to speculate whether deterioration of cognitive function and mental deterioration observed during advanced tuberculosis of the CNS is associated with impairment of neuronal function as a direct consequence of *M. tuberculosis* bacillus uptake.

In summary, conclusive evidence that *M. tuberculosis* has the necessary capacity to infect neurons is provided. The implications of neuronal infection, the effect on neuronal function, and the influence exerted on the intercellular interactions during host immune responses against tuberculosis need further investigation and should be examined.

ACKNOWLEDGMENTS

We thank Marylin Tyler and Lizette Fick for their contributions to the histopathology, Lester Davids and Toni Wiggins for their help in acquiring the SK-N-SH cell line, and especially Faried Abbass for technical support. We thank the staff of the Division of Immunology and the Animal Unit at UCT for their contributions to animal care and technical support.

This study was supported by the National Research Foundation (South Africa), Deutscher Akademischer Austausch Dienst (Germany), the Medical Research Council (South Africa), and the University of Cape Town and National Health and Laboratory Service (South Africa).

REFERENCES

1. **WHO.** 2012. Global tuberculosis control 2011. WHO, Geneva, Switzerland.
2. **Be NA, Kim KS, Bishai WR, Jain SK.** 2009. Pathogenesis of central nervous system tuberculosis. Curr. Mol. Med. **9:**94–99. http://dx.doi.org/10.2174/156652409787581655.
3. **Kingkaew N, Sangtong B, Amnuaiphon W, Jongpaibulpatana J, Mankatittham W, Akksilp S, Sirinak C, Nateniyom S, Burapat C, Kittikraisak W, Monkongdee P, Varma JK.** 2009. HIV-associated extrapulmonary tuberculosis in Thailand: epidemiology and risk factors for death. Int. J. Infect. Dis. **13:**722–729. http://dx.doi.org/10.1016/j.ijid.2008.11.013.
4. **Sharma SK, Mohan A, Kadhiravan T.** 2005. HIV-TB co-infection: epidemiology, diagnosis, and management. Indian J. Med. Res. **121:**550–567.
5. **Donald PR, Schaaf HS, Schoeman JF.** 2005. Tuberculous meningitis and miliary tuberculosis: the Rich focus revisited. J. Infect. **50:**193–195. http://dx.doi.org/10.1016/j.jinf.2004.02.010.
6. **Jain SK, Paul-Satyaseela M, Lamichhane G, Kim KS, Bishai WR.** 2006. Mycobacterium tuberculosis invasion and traversal across an in vitro human blood-brain barrier as a pathogenic mechanism for central nervous system tuberculosis. J. Infect. Dis. **193:**1287–1295. http://dx.doi.org/10.1086/502631.
7. **Rich A, McCordick H.** 1933. The pathogenesis of tuberculous meningitis. Bull. John Hopkins Hosp. **52:**5–37.
8. **Garcia-Perez BE, Mondragon-Flores R, Luna-Herrera J.** 2003. Internalization of Mycobacterium tuberculosis by macropinocytosis in nonphagocytic cells. Microb. Pathog. **35:**49–55. http://dx.doi.org/10.1016/S0882-4010(03)00089-5.
9. **Munoz S, Rivas-Santiago B, Enciso JA.** 2009. Mycobacterium tuberculosis entry into mast cells through cholesterol-rich membrane microdomains. Scand. J. Immunol. **70:**256–263. http://dx.doi.org/10.1111/j.1365-3083.2009.02295.x.
10. **Teitelbaum R, Schubert W, Gunther L, Kress Y, Macaluso F, Pollard JW, McMurray DM, Bloom BR.** 1999. The M cell as a portal of entry to the lung for the bacterial pathogen Mycobacterium tuberculosis. Immunity **10:**641–650. http://dx.doi.org/10.1016/S1074-7613(00)80063-1.
11. **Wolf AJ, Linas B, Trevejo-Nunez GJ, Kincaid E, Tamura T, Takatsu K, Ernst JD.** 2007. Mycobacterium tuberculosis infects dendritic cells with high frequency and impairs their function in vivo. J. Immunol. **179:**2509–2519.
12. **Giacomini E, Iona E, Ferroni L, Miettinen M, Fattorini L, Orefici G, Julkunen I, Coccia EM.** 2001. Infection of human macrophages and dendritic cells with Mycobacterium tuberculosis induces a differential cytokine gene expression that modulates T cell response. J. Immunol. **166:**7033–7041.
13. **Hickman SP, Chan J, Salgame P.** 2002. Mycobacterium tuberculosis induces differential cytokine production from dendritic cells and macrophages with divergent effects on naive T cell polarization. J. Immunol. **168:**4636–4642.
14. **Barrios-Payan J, Saqui-Salces M, Jeyanathan M, Vazquez AA, Arreola MC, Rook G, Hernandez-Pando R.** 2012. Extrapulmonary location of Mycobacterium tuberculosis DNA during latent infection. J. Infect. Dis. **206:**1194–1205. http://dx.doi.org/10.1093/infdis/jis381.
15. **Arruda S, Bomfim G, Knights R, Huima-Byron T, Riley LW.** 1993. Cloning of an M. tuberculosis DNA fragment associated with entry and survival inside cells. Science **261:**1454–1457. http://dx.doi.org/10.1126/science.8367727.
16. **Chitale S, Ehrt S, Kawamura I, Fujimura T, Shimono N, Anand N, Lu S, Cohen-Gould L, Riley LW.** 2001. Recombinant Mycobacterium tuberculosis protein associated with mammalian cell entry. Cell. Microbiol. **3:**247–254. http://dx.doi.org/10.1046/j.1462-5822.2001.00110.x.
17. **Drevets DA, Leenen PJ, Greenfield RA.** 2004. Invasion of the central nervous system by intracellular bacteria. Clin. Microbiol. Rev. **17:**323–347. http://dx.doi.org/10.1128/CMR.17.2.323-347.2004.
18. **Peterson PK, Gekker G, Hu S, Sheng WS, Anderson WR, Ulevitch RJ, Tobias PS, Gustafson KV, Molitor TW, Chao CC.** 1995. CD14 receptor-mediated uptake of nonopsonized Mycobacterium tuberculosis by human microglia. Infect. Immun. **63:**1598–1602.
19. **Rock RB, Hu S, Gekker G, Sheng WS, May B, Kapur V, Peterson PK.** 2005. Mycobacterium tuberculosis-induced cytokine and chemokine expression by human microglia and astrocytes: effects of dexamethasone. J. Infect. Dis. **192:**2054–2058. http://dx.doi.org/10.1086/498165.
20. **Yang CS, Lee HM, Lee JY, Kim JA, Lee SJ, Shin DM, Lee YH, Lee DS, El-Benna J, Jo EK.** 2007. Reactive oxygen species and p47phox activation are essential for the Mycobacterium tuberculosis-induced pro-inflammatory response in murine microglia. J. Neuroinflammation **4:**27. http://dx.doi.org/10.1186/1742-2094-4-27.
21. **Peterson PK, Hu S, Anderson WR, Chao CC.** 1994. Nitric oxide production and neurotoxicity mediated by activated microglia from human versus mouse brain. J. Infect. Dis. **170:**457–460. http://dx.doi.org/10.1093/infdis/170.2.457.
22. **Rambukkana A, Salzer JL, Yurchenco PD, Tuomanen EI.** 1997. Neural targeting of Mycobacterium leprae mediated by the G domain of the laminin-alpha2 chain. Cell **88:**811–821. http://dx.doi.org/10.1016/S0092-8674(00)81927-3.
23. **Aung T, Kitajima S, Nomoto M, En J, Yonezawa S, Arikawa I, Goto M.** 2007. Mycobacterium leprae in neurons of the medulla oblongata and spinal cord in leprosy. J. Neuropathol. Exp. Neurol. **66:**284–294. http://dx.doi.org/10.1097/nen.0b013e31803d597e.
24. **Jin Y, Dons L, Kristensson K, Rottenberg ME.** 2001. Neural route of cerebral Listeria monocytogenes murine infection: role of immune response mechanisms in controlling bacterial neuroinvasion. Infect. Immun. **69:**1093–1100. http://dx.doi.org/10.1128/IAI.69.2.1093-1100.2001.
25. **Jin Y, Lundkvist G, Dons L, Kristensson K, Rottenberg ME.** 2004. Interferon-gamma mediates neuronal killing of intracellular bacteria. Scand. J. Immunol. **60:**437–448. http://dx.doi.org/10.1111/j.0300-9475.2004.01500.x.
26. **Bowen S, Ateh DD, Deinhardt K, Bird MM, Price KM, Baker CS, Robson JC, Swash M, Shamsuddin W, Kawar S, El-Tawil T, Roos J, Hoyle A, Nickols CD, Knowles CH, Pullen AH, Luthert PJ, Weller RO, Hafezparast M, Franklin RJ, Revesz T, King RH, Berninghausen O, Fisher EM, Schiavo G, Martin JE.** 2007. The phagocytic capacity of neurones. Eur. J. Neurosci. **25:**2947–2955. http://dx.doi.org/10.1111/j.1460-9568.2007.05554.x.
27. **Giulian D, Baker TJ.** 1986. Characterization of ameboid microglia isolated from developing mammalian brain. J. Neurosci. **6:**2163–2178.
28. **Saura J, Tusell JM, Serratosa J.** 2003. High-yield isolation of murine microglia by mild trypsinization. Glia **44:**183–189. http://dx.doi.org/10.1002/glia.10274.
29. **Ahlemeyer B, Baumgart-Vogt E.** 2005. Optimized protocols for the simultaneous preparation of primary neuronal cultures of the neocortex, hippocampus and cerebellum from individual newborn (P0.5) C57Bl/6J mice. J. Neurosci. Methods **149:**110–120. http://dx.doi.org/10.1016/j.jneumeth.2005.05.022.
30. **Brewer GJ, Torricelli JR, Evege EK, Price PJ.** 1993. Optimized survival of hippocampal neurons in B27-supplemented Neurobasal, a new serum-free medium combination. J. Neurosci. Res. **35:**567–576. http://dx.doi.org/10.1002/jnr.490350513.
31. **Kaech S, Banker G.** 2006. Culturing hippocampal neurons. Nat. Protoc. **1:**2406–2415. http://dx.doi.org/10.1038/nprot.2006.356.
32. **Jain P, Cerone MA, Leblanc AC, Autexier C.** 2007. Telomerase and neuronal marker status of differentiated NT2 and SK-N-SH human neuronal cells and primary human neurons. J. Neurosci. Res. **85:**83–89. http://dx.doi.org/10.1002/jnr.21094.
33. **LePage KT, Dickey RW, Gerwick WH, Jester EL, Murray TF.** 2005. On the use of neuro-2a neuroblastoma cells versus intact neurons in primary culture for neurotoxicity studies. Crit. Rev. Neurobiol. **17:**27–50. http://dx.doi.org/10.1615/CritRevNeurobiol.v17.i1.20.
34. **Shams H, Wizel B, Lakey DL, Samten B, Vankayalapati R, Valdivia RH, Kitchens RL, Griffith DE, Barnes PF.** 2003. The CD14 receptor does not mediate entry of Mycobacterium tuberculosis into human mononuclear phagocytes. FEMS Immunol. Med. Microbiol. **36:**63–69. http://dx.doi.org/10.1016/S0928-8244(03)00039-7.
35. **Peltier DC, Simms A, Farmer JR, Miller DJ.** 2010. Human neuronal cells possess functional cytoplasmic and TLR-mediated innate immune pathways influenced by phosphatidylinositol-3 kinase signaling. J. Immunol. **184:**7010–7021. http://dx.doi.org/10.4049/jimmunol.0904133.
36. **Kigerl KA, Lai W, Rivest S, Hart RP, Satoskar AR, Popovich PJ.** 2007. Toll-like receptor (TLR)-2 and TLR-4 regulate inflammation, gliosis, and myelin sparing after spinal cord injury. J. Neurochem. **102:**37–50. http://dx.doi.org/10.1111/j.1471-4159.2007.04524.x.
37. **Tang SC, Arumugam TV, Xu X, Cheng A, Mughal MR, Jo DG, Lathia JD, Siler DA, Chigurupati S, Ouyang X, Magnus T, Camandola S, Mattson MP.** 2007. Pivotal role for neuronal Toll-like receptors in isch-

emic brain injury and functional deficits. Proc. Natl. Acad. Sci. U. S. A **104:**13798–13803. http://dx.doi.org/10.1073/pnas.0702553104.
38. **Abel B, Thieblemont N, Quesniaux VJ, Brown N, Mpagi J, Miyake K, Bihl F, Ryffel B.** 2002. Toll-like receptor 4 expression is required to control chronic Mycobacterium tuberculosis infection in mice. J. Immunol. **169:**3155–3162.
39. **Drennan MB, Nicolle D, Quesniaux VJ, Jacobs M, Allie N, Mpagi J, Fremond C, Wagner H, Kirschning C, Ryffel B.** 2004. Toll-like receptor 2-deficient mice succumb to Mycobacterium tuberculosis infection. Am. J. Pathol. **164:**49–57. http://dx.doi.org/10.1016/S0002-9440(10)63095-7.
40. **Welin A, Lerm M.** 2012. Inside or outside of phagosome? The controversy of the intracellular localization of Mycobacterium tuberculosis. Tuberculosis **92:**113–120. http://dx.doi.org/10.1016/j.tube.2011.09.009.
41. **Esposito C, Marasco D, Delogu G, Pedone E, Berisio R.** 2011. Heparin-binding hemagglutinin HBHA from Mycobacterium tuberculosis affects actin polymerisation. Biochem. Biophys. Res. Commun. **410:**339–344. http://dx.doi.org/10.1016/j.bbrc.2011.05.159.
42. **Lasunskaia EB, Campos MN, de Andrade MR, Damatta RA, Kipnis TL, Einicker-Lamas M, Da Silva WD.** 2006. Mycobacteria directly induce cytoskeletal rearrangements for macrophage spreading and polarization through TLR2-dependent PI3K signaling. J. Leukoc. Biol. **80:**1480–1490. http://dx.doi.org/10.1189/jlb.0106066.
43. **Bermudez LE, Goodman J.** 1996. Mycobacterium tuberculosis invades and replicates within type II alveolar cells. Infect. Immun. **64:**1400–1406.
44. **Anes E, Kühnel MP, Bos E, Moniz-Pereira J, Habermann A, Griffiths G.** 2003. Selected lipids activate phagosome actin assembly and maturation resulting in killing of pathogenic mycobacteria. Nat. Cell Biol. **5:**793–802. http://dx.doi.org/10.1038/ncb1036.
45. **Kolonko M, Geffken AC, Blumer T, Hagens K, Schaible UE, Hagedorn M.** 2013. WASH-driven actin polymerization is required for efficient mycobacterial phagosome maturation arrest. Cell. Microbiol. http://dx.doi.org/10.1111/cmi.12217.
46. **Polazzi E, Monti B.** 2010. Microglia and neuroprotection: from in vitro studies to therapeutic applications. Prog. Neurobiol. **92:**293–315. http://dx.doi.org/10.1016/j.pneurobio.2010.06.009.
47. **Keane J, Remold HG, Kornfeld H.** 2000. Virulent Mycobacterium tuberculosis strains evade apoptosis of infected alveolar macrophages. J. Immunol. **164:**2016–2020.
48. **Neumann H, Cavalie A, Jenne DE, Wekerle H.** 1995. Induction of MHC class I genes in neurons. Science **269:**549–552. http://dx.doi.org/10.1126/science.7624779.
49. **Berenguer J, Moreno S, Laguna F, Vicente T, Adrados M, Ortega A, Gonzalez-LaHoz J, Bouza E.** 1992. Tuberculous meningitis in patients infected with the human immunodeficiency virus. N. Engl. J. Med. **326:**668–672. http://dx.doi.org/10.1056/NEJM199203053261004.
50. **Silber E, Sonnenberg P, Ho KC, Koornhof HJ, Eintracht S, Morris L, Saffer D.** 1999. Meningitis in a community with a high prevalence of tuberculosis and HIV infection. J. Neurol. Sci. **162:**20–26. http://dx.doi.org/10.1016/S0022-510X(98)00259-7.
51. **El Sahly HM, Teeter LD, Pan X, Musser JM, Graviss EA.** 2007. Mortality associated with central nervous system tuberculosis. J. Infect. **55:**502–509. http://dx.doi.org/10.1016/j.jinf.2007.08.008.
52. **Puccioni-Sohler M, Brandao CO.** 2007. Factors associated to the positive cerebrospinal fluid culture in the tuberculous meningitis. Arq. Neuropsiquiatr. **65:**48–53. http://dx.doi.org/10.1590/S0004-282X2007000100011.
53. **Caruso AM, Serbina N, Klein E, Triebold K, Bloom BR, Flynn JL.** 1999. Mice deficient in CD4 T cells have only transiently diminished levels of IFN-gamma, yet succumb to tuberculosis. J. Immunol. **162:**5407–5416.